PHYSICAL REVIEW A **86**, 011401(R) (2012)

Dependence of high-order-harmonic-generation yield on driving-laser ellipticity

Max Möller,[1,2,3] Yan Cheng,[3] Sabih D. Khan,[4] Baozhen Zhao,[5] Kun Zhao,[3] Michael Chini,[3] Gerhard G. Paulus,[1,2,6] and Zenghu Chang[3,*]

[1]*Institut für Optik und Quantenelektronik, Friedrich-Schiller Universität Jena, 07743 Jena, Germany*
[2]*Helmholtz Institut Jena, Helmholtzweg 4, 07743 Jena, Germany*
[3]*CREOL and Department of Physics, University of Central Florida, Orlando, Florida 32816, USA*
[4]*Department of Physics, Kansas State University, Manhattan, Kansas 66506, USA*
[5]*Department of Physics and Astronomy, University of Nebraska-Lincoln, Lincoln, Nebraska 68588, USA*
[6]*Department of Physics, Texas A&M University, College Station, Texas 77843, USA*

(Received 23 April 2012; published 26 July 2012)

High-order-harmonic-generation yield is remarkably sensitive to driving laser ellipticity, which is interesting from a fundamental point of view as well as for applications. The most well-known example is the generation of isolated attosecond pulses via polarization gating. We develop an intuitive semiclassical model that makes use of the recently measured initial transverse momentum of tunneling ionization. The model is able to predict the dependence of the high-order-harmonic yield on driving laser ellipticity and is in good agreement with experimental results and predictions from a numerically solved time-dependent Schrödinger equation.

DOI: 10.1103/PhysRevA.86.011401 PACS number(s): 32.80.Wr, 42.65.−k, 33.20.Xx

High-order-harmonic generation (HHG) in gases is presently the most important method for generating extreme ultraviolet (XUV) attosecond pulses from intense infrared lasers [1,2]. The semiclassical picture of HHG divides the process into three steps that take place within less than an optical cycle [3,4]. First, the single active electron is ionized from the bound state to the continuum. During the second step, the electron travels in the continuum influenced by the laser field. The XUV photon emission takes place in the third step when the electron is driven back to the parent ion and recombines about half an optical cycle after the initial ionization. The ionization step is fundamental for the behavior of the entire HHG process. Typically, it is treated by tunneling of a bound single active electron through a quasistatic potential barrier arising from the superposition of the Coulomb field and the strong laser field [5]. This model of tunneling at optical frequencies has been under experimental [6] and theoretical investigation over the past years [7,8]. Here, we develop a semiclassical model that qualitatively and quantitatively explains the dependence of high-order-harmonic-generation yield on driving laser ellipticity based on the transverse velocity distribution of the electron wave packet at the exit of the tunnel. The model utilizes classical mechanics to reveal the subcycle electron dynamics in an elliptically polarized laser field [9].

Our results can be used to design and further optimize techniques to generate isolated attosecond laser pulses from multicycle driving lasers which emit attosecond XUV pulses each half cycle of the driving laser, i.e., separated by only about 1 fs in time, unless specific technical measures are taken. An obvious way for generating isolated attosecond pulses is the use of driving laser pulses consisting of essentially a single optical cycle [10]. The construction of such quasi-single-cycle lasers is quite demanding [11]. This holds in particular if a high driving laser pulse energy (>100 mJ), which has a positive impact on HHG flux, is a prime design criterion. An alternative approach to generate isolated attosecond pulses is to manipulate conventional multicycle laser pulses such that only a single optical cycle can contribute to HHG. The basis for most of such methods is the remarkable sensitivity of HHG efficiency on driving laser ellipticity. Thus, by tailoring the polarization such that only a single optical cycle contributes to HHG, it is also possible to produce isolated attosecond pulses. This technique is known as polarization gating (PG) [12,13]. Since its proposal in 1994 [14], polarization gating has become a frequently used technique. In fact, a variety of innovations for such gating methods have expanded their range of applicability. Examples are interferometric PG [15], double optical gating [16,17], and generalized double optical gating [18] (see Ref. [19] for a review).

However, the decisive physical effect is still the dependence of high-order-harmonic yield on driving laser ellipticity [20,21]. Our semiclassical model identifies the physical mechanism of the ellipticity dependence in HHG. A parametric study of the effect performed at 810 and 405 nm driving laser wavelength as well as experimental and theoretical results from the literature are found to be in good agreement with the model. As the analysis allows calculating the ellipticity dependence of the yield in HHG as a function of the driving laser wavelength, intensity, target atom, and harmonic order, it should be very useful for designing polarization gating-based schemes for the generation of isolated attosecond pulses from multicycle driving lasers.

As briefly introduced, the semiclassical theory of HHG is based on the analysis of classical electron trajectories that evolve when atoms release electrons in a strong oscillating electric field. Of particular interest are those trajectories that return to the parent ion core. Since the kinetic energy of the returning electron can exceed the photon energy of the driving laser field by orders of magnitude, recombination will lead to the emission of extreme ultraviolet photons. This already suggests the explanation for the strong dependence of

*To whom correspondence should be addressed: zenghu.chang@ucf.edu

high-order-harmonic yield on driving laser ellipticity. One of the transverse components of the elliptically polarized field will prevent the electrons from returning to the ion core and thus switch off the mechanism of HHG.

For a quantitative analysis, quantum features of the ionization process have to be taken into account. The respective semiclassical model of the ellipticity dependence of HHG is based on the assumption that the HHG radiation is due to electron trajectories where the transverse displacement caused by the external field is compensated by an initial transverse velocity of the electron at the exit of the tunnel. Electrons following these trajectories (which lead exactly back to the ion core) have a higher probability of recombination with the parent ion and emission of an HHG photon than trajectories missing the ion core.

The trajectories favorable for HHG can be found easily when the Coulomb field of the ion is neglected. Integrating the equations of motion for a free electron in an elliptically polarized laser field that is approximated as a monochromatic plane wave, $\vec{F}(t) = F/\sqrt{1+\varepsilon^2}[\cos\omega t; \varepsilon \sin\omega t]$, with ellipticity ε, amplitude F, and frequency ω, yields the trajectory,

$$\begin{aligned}\vec{r} = &-\frac{F}{\sqrt{1+\varepsilon^2}}\frac{1}{\omega^2}\\ &\times\begin{bmatrix}-\cos\omega t + \cos\omega t_0 - \omega\,(t-t_0)\sin\omega t_0\\ \varepsilon\,(-\sin\omega t + \sin\omega t_0 + \omega\,(t-t_0)\cos\omega t_0)\end{bmatrix}\\ &+(t-t_0)\begin{bmatrix}v_{x0}\\ v_{y0}\end{bmatrix}. \end{aligned} \tag{1}$$

Here, in the spirit of the semiclassical strong-field model, the initial positions x_0 and y_0 are set to zero and t_0 denotes the time of ionization. Atomic units are used except where noted.

The angle between the ionizing field vector and the coordinate axis at the time of ionization is given by $\alpha_0 = \tan^{-1}[\varepsilon \tan(\omega t_0)]$. A rotation $\boldsymbol{R}(-\alpha_0)$ is applied to express the initial velocities v_{x0} and v_{y0} in terms of parallel and transverse velocities to the ionizing field vector, $v_\parallel$ and $v_\perp$,

$$\begin{bmatrix}v_{x0}\\ v_{y0}\end{bmatrix} = \boldsymbol{R}(-\alpha_0)\begin{bmatrix}v_\parallel\\ v_\perp\end{bmatrix} = \begin{bmatrix}v_\parallel\cos(\alpha_0) + v_\perp\sin(\alpha_0)\\ -v_\parallel\sin(\alpha_0) + v_\perp\cos(\alpha_0)\end{bmatrix}. \tag{2}$$

As the electron leaves the atom by tunneling, we assume that the initial velocity parallel to the ionizing field is zero, $v_\parallel = 0$.

For nonzero ellipticity ε and zero initial velocity $v_\parallel = v_\perp = 0$, the electron can never return to the parent ion at the origin. Consequently, high-order-harmonic emission is avoided, as illustrated in Fig. 1(a). However, a return at a later recombination time, $t_r > t_0$, can be achieved if the trajectory is launched with a finite initial velocity $v_\perp$ perpendicular to the field direction at $t = t_0$. This idea was stressed, e.g., in the trajectory analysis for laser fields with a polarization gate [22,23]. For a given starting time, the return time t_r can be found by solving the condition of return $\vec{r}\,(t_r) = 0$, which yields [24]

$$\begin{aligned}&(\varepsilon^2+1)\omega(t_r-t_0)\sin\omega t_0\cos\omega t_0\\ &-\varepsilon^2\sin\omega t_0(\sin\omega t_r - \sin\omega t_0)\\ &+\cos\omega t_0(\cos\omega t_r - \cos\omega t_0) = 0.\end{aligned} \tag{3}$$

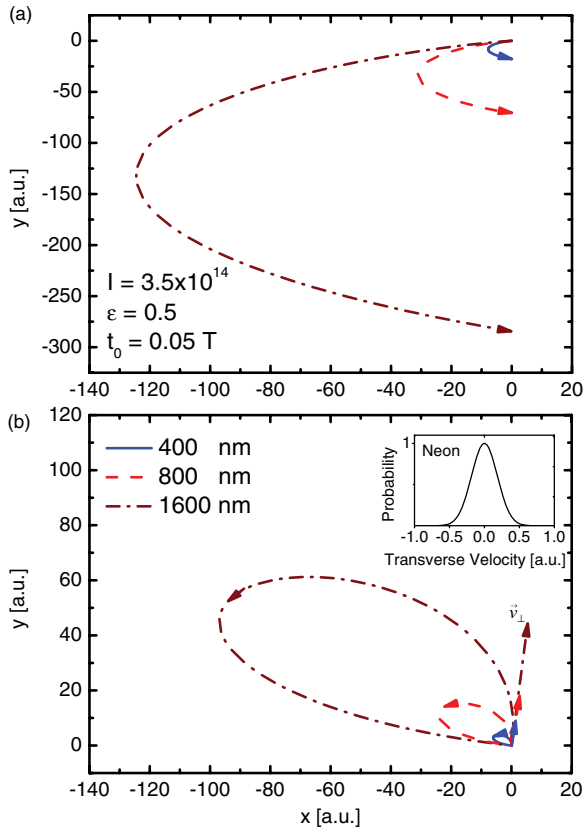

FIG. 1. (Color online) (a) Electron trajectories in elliptically polarized fields driven at different wavelengths. The trajectories start at the instant of ionization, here $t_0 = 0.05T$, and terminate when the electron crosses the x axis. The movement along the minor field component causes a displacement which easily reaches tens of atomic units and is proportional to the square of the wavelength, $\propto \lambda^2$. (b) Electron trajectories where an initial transverse velocity $\vec{v}_\perp$ (indicated by the arrows) compensates the displacement, thus facilitating the return of the trajectory to the origin. The inset shows the probability distribution for an initial transverse velocity for neon at an intensity of 3.5×10^{14} W/cm^2.

The required initial velocity $v_\perp$ then is given by

$$v_\perp = -\frac{F\varepsilon}{\sqrt{1+\varepsilon^2}}\frac{1}{\omega\cos\alpha_0}\left(\frac{\sin\omega t_r - \sin\omega t_0}{\omega\,(t_r - t_0)} - \cos\omega t_0\right). \tag{4}$$

The resulting trajectory with the initial perpendicular velocity is adjusted such that the trajectory immediately returns to the ion core, as shown in Fig. 1(b).

Although a suitable transverse initial electron velocity facilitates the collision of the returning electron with the ion and thus increases the probability of recombination, one also has to take into account that electrons leaving the tunnel are unlikely to have large transverse velocities [5–8]. This changes the probability of finding such an electron trajectory, as can be seen from the inset in Fig. 1(b). The ellipticity-dependent yield of high-order harmonics normalized to the yield with a linearly polarized laser is therefore

$$\frac{I_{\mathrm{XUV}}(\varepsilon)}{I_{\mathrm{XUV}}(\varepsilon=0)} \approx \frac{w\,(v_\perp)}{w\,(v_\perp=0)} = \exp\left(-\frac{\sqrt{2I_p}v_\perp(\varepsilon)^2}{|F(t_0)|}\right), \tag{5}$$

where $w(v_\perp)$ is the perpendicular velocity distribution that was predicted by tunneling theory [8] and found to agree well with experimental results [6]. Here, I_p denotes the ionization potential and $|F(t_0)|$ is the absolute value of the driving field at the instant of ionization.

In order to calculate the yield of high-order-harmonic radiation at a given ellipticity, one identifies t_r for all t_0 in the first quarter of the optical cycle ($0 < t_0 < T/4$) by solving Eq. (3) numerically, considering only the first quarter cycle is sufficient due to the driving laser field's periodicity. In fact, Eq. (3) has in general several solutions t_r which are related to different $v_\perp$ by Eq. (4). For HHG, however, only the first return of the electron to the ion is relevant, i.e., only the solution with the smallest t_r needs to be taken into account. According to the classical model of HHG, the photon energy that is emitted by a trajectory starting at t_0 is given by the electron's kinetic energy upon its return at t_r plus the ionization energy of the target atom I_p. Similar to the case of linear polarization, there are two types of trajectories that lead to identical photon energy but have a different starting time t_0, return time t_r, and initial velocity $v_\perp$ [25]. In the literature, they are known as short and long trajectories. It is also known that harmonics generated by long trajectories have undesirable phase-matching properties, which is why experimental conditions are usually chosen such that only the short trajectories contribute to the observed harmonics. Thus, we calculate the ellipticity-dependent yield using Eq. (5) for the short trajectories.

An analytical expression for the ellipticity-dependent yield can be derived based on the following assumptions: (i) A small ellipticity ($\varepsilon^2 \ll 1$) which results in $\sqrt{1+\varepsilon^2} \approx 1$. This is reasonable as the yield drops quickly as ε is increased, particularly at longer driving laser wavelengths. (ii) Photon energies that are close to the cutoff are related to starting times shortly after the field reached a maximum. Therefore, one can neglect the rotation of the field vector at the instant of ionization, $\cos\alpha_0 = \cos\{\tan^{-1}[\varepsilon\tan(\omega t_0)]\} \approx 1$, in Eq. (4). With the same argument, one approximates $|F(t_0)| \approx \sqrt{I}$ in Eq. (5), where I is the peak intensity of the field. (iii) Using (i) and (ii) one can write Eq. (4) as $v_\perp = -\beta F\varepsilon\lambda/2\pi c$, where $\beta = (\frac{\sin\omega t_r - \sin\omega t_0}{\omega(t_r - t_0)} - \cos\omega t_0)$. c is the speed of light and λ denotes the laser wavelength. β depends on the harmonic order of interest and within the approximations (i) and (ii), it can be calculated using closed-form analytical solutions for linear polarization [26].

The resulting ellipticity-dependent yield is approximately a Gaussian function which results directly from the velocity spreading of the electron wave packet at the exit of the tunnel,

$$\frac{I_{\mathrm{XUV}}(\varepsilon)}{I_{\mathrm{XUV}}(\varepsilon=0)} \approx \exp\left(-\frac{\beta^2\sqrt{2I_pI}}{4\pi^2c^2}\lambda^2\varepsilon^2\right). \tag{6}$$

The Gaussian dependence of high-order-harmonic yield on ellipticity ε reflects the Gaussian dependence of the ionization probability on $v_\perp$. This emphasizes that high-order-harmonic radiation from an elliptical polarized laser field comes from electron trajectories where the transverse displacement is compensated by an initial transverse velocity.

For the design of optical gating schemes, the threshold ellipticity $\varepsilon_{\mathrm{th}}$ is of particular interest as this quantity determines the amplitude of satellite pulses that arise from radiation generated outside the polarization gate [12]. Here, we choose $\varepsilon_{\mathrm{th}}$ as the ellipticity where the normalized yield drops to 0.1. For cutoff harmonics, where $\beta^2 \approx 1.59$, one finds

$$\varepsilon_{\mathrm{th}} \approx \frac{691}{I_p^{1/4}}\frac{1}{I^{1/4}}\frac{1}{\lambda}. \tag{7}$$

Equation (7) shows a $1/\lambda$ scaling as was found experimentally [27] and theoretically based on time-dependent Schrödinger equation (TDSE) simulations [28].

The predictions of the model are compared with measurements of the ellipticity-dependent high-order-harmonic yield in using 405- and 810-nm driving lasers. We used the setup that was presented in Ref. [29]. The 810-nm, 30-fs, 4.8-mJ pulses were frequency doubled in a 300-μm beta barium borate crystal (type I phase matching) to produce 0.9-mJ pulses of second harmonic radiation centered at 405 nm. Two dichroic mirrors removed the fundamental radiation. The ellipticity was controlled by a combination of a zero-order half-wave plate and a quarter-wave plate such that the orientation of the polarization ellipse did not change as the ellipticity was changed. This minimizes the influence of the polarization-dependent diffraction efficiency of the toroidal grating in the XUV spectrometer. The pulses were focused into a 1-mm-long gas cell using a 375-mm silver-coated concave mirror at near normal incidence. The fundamental radiation was blocked by a 300-nm aluminum filter before the XUV spectrometer. The ellipticity-dependent yield from 810-nm driving laser pulses was measured using the same setup but with optics that were designed for 810 nm.

In Fig. 2, experimental results from neon and helium are compared with corresponding theoretical results. The numerical results match the experiments quite well, while the analytical results show the qualitative trend but larger quantitative deviations for plateau harmonic orders far from the cutoff. This is expected due to the breakdown of the aforementioned assumptions. In particular, neglecting effects due the rotated field vector at t_0 and assuming starting times that are close to the maximum of the field fail for low-energy plateau harmonics.

To further validate the model, the threshold ellipticities $\varepsilon_{\mathrm{th}}$ of different harmonic orders at 810 and 405 nm are examined in Figs. 3(a) and 3(b). The theory matches the trend that higher harmonic orders are more susceptible to the ellipticity and therefore have lowered threshold ellipticity. This finding has implications for the design of polarization-based gating schemes.

The threshold ellipticity of the 11th harmonic of 405 nm as a function of intensity is shown in Fig. 3(c). Theory and experiment show that higher intensity results in a narrower ellipticity dependence and thus a smaller threshold ellipticity. Higher intensity causes a larger excursion amplitude of the trajectory and therefore requires a larger initial transverse velocity for the trajectory to return. However, the width of the transverse velocity distribution is also increased, as evident from Eq. (5). This mutual compensation explains why the intensity has a relatively weak influence on the threshold ellipticity.

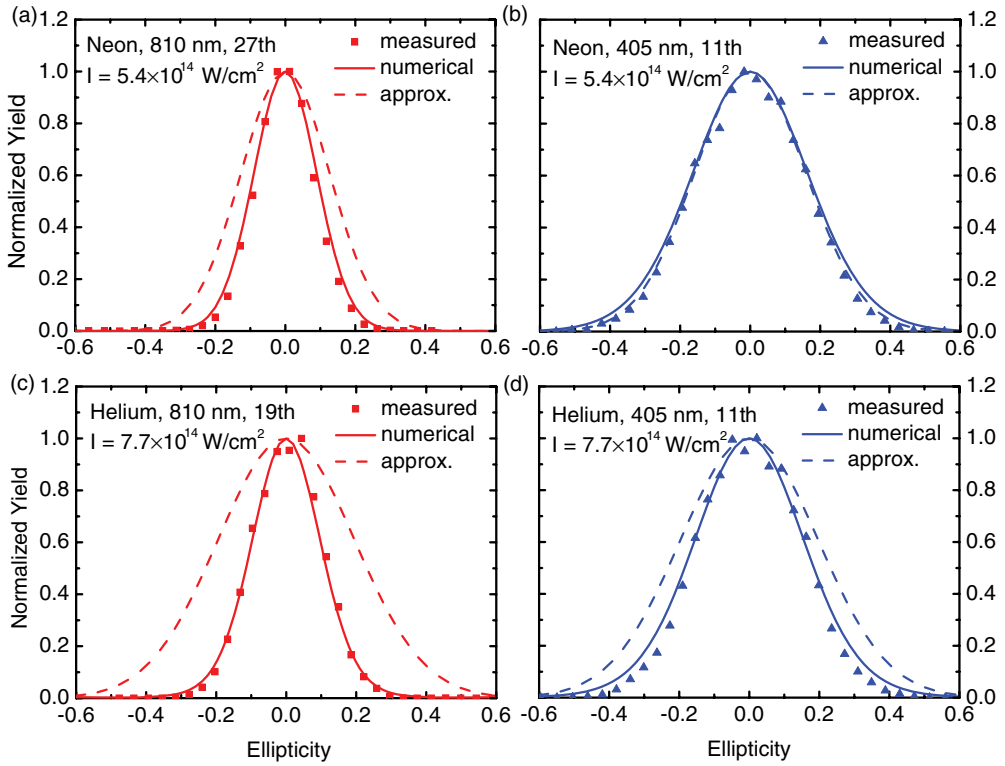

FIG. 2. (Color online) Comparison between measured data (data points) and results obtained by numerical (solid lines) and analytical calculation (dashed lines) at the conditions of the experiment. Numerical and experimental data agree very well while the analytical approximation shows deviations which become larger the more the harmonic's energy differs from the cutoff energy. The ratio between the observed harmonic energy and the cutoff energy is (a) 0.27, (b) 0.39, (c) 0.25, and (d) 0.29.

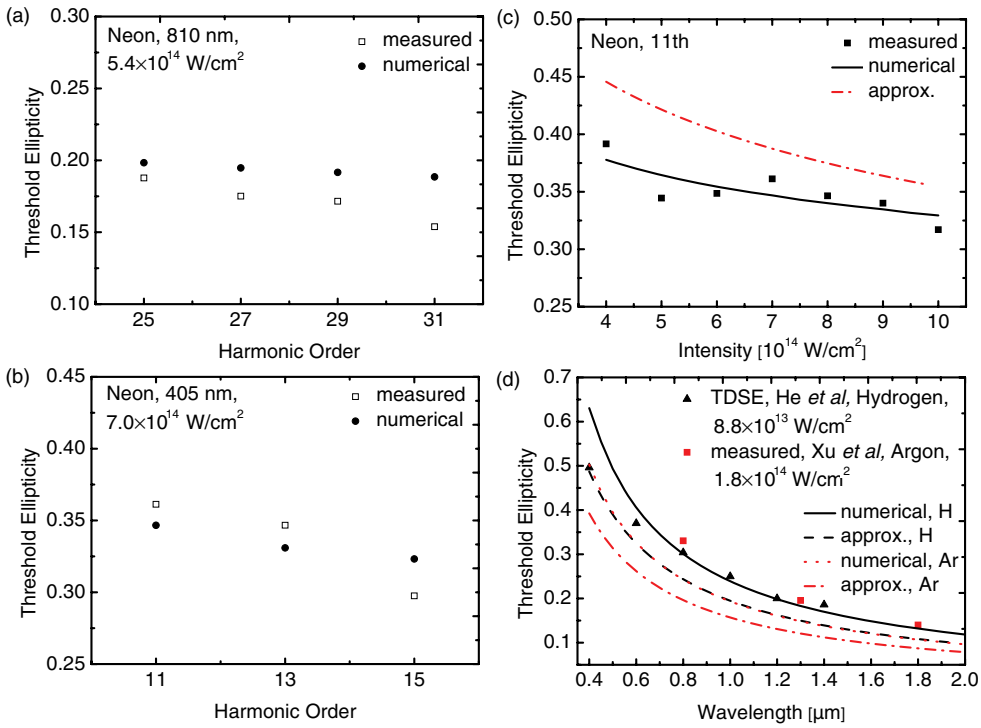

FIG. 3. (Color online) Threshold ellipticity ε_{th} as a function of harmonic order for (a) 810-nm and (b) 405-nm driving laser wavelengths, (c) intensity, and (d) wavelength. Each data point was obtained by fitting a Gaussian to the ellipticity dependence and calculating the threshold ellipticity from the fit parameters. The threshold ellipticity is weakly susceptible to the harmonic order and intensity. Increasing the driving laser wavelength reduces the threshold ellipticity, which makes long wavelengths attractive for the polarization-based gating schemes.

The wavelength scaling of the threshold ellipticity is investigated in Fig. 3(d). The results of the semiclassical model agree quite well with the TDSE simulations performed for hydrogen [28]. The experiments performed in argon [27] show an offset as compared to the semiclassical model. For the design of polarization-based gating schemes, a smaller threshold ellipticity observed for longer wavelengths reduces the demands on the shortness of the driving laser pulse duration.

The deviations between the semiclassical model and the experiments are less than 20%. These differences might come from a too large width of the perpendicular velocity distribution, as it was found in Ref. [6], or originate for the parent ion's influence on the electron wave packet. However, they can also have their origin from propagation and phase-matching effects in the HHG process which are not included in the model. Increasing the ellipticity, for example, lowers the peak field strength and therefore affects the free-electron density. This changes the propagation of the generated harmonic radiation as well as the propagation of the driving laser pulse.

In conclusion, we have shown that high-order-harmonic radiation generated in an elliptically polarized laser field comes from electron trajectories where the transverse displacement is compensated by an initial transverse velocity at the instant of ionization. As these electron trajectories have a lower tunneling probability, the HHG yield decreases as ellipticity increases. This semiclassical model of the ellipticity-dependent yield in HHG intuitively explains the susceptibility of HHG to the ellipticity of the driving laser as a direct consequence of the structure electron wave packet at the exit of the tunnel. Good agreement with experimental and previous theoretical results was demonstrated. Simple approximate analytical expressions can be used to estimate the ellipticity-dependent yield for cutoff harmonics, as a function of wavelength, intensity, and ionization potential of the target atom. The results of such an analysis can be used to design and optimize optical gating schemes for any driving laser wavelength.

This material is supported by the US Army Research Office, by the US Department of Energy, by the National Science Foundation, by the German Science Foundation (DFG PA730/4), and by Laserlab Europe.

[1] P. B. Corkum and F. Krausz, Nat. Phys. **3**, 381 (2007).
[2] F. Krausz and M. Ivanov, Rev. Mod. Phys. **81**, 163 (2009).
[3] P. B. Corkum, Phys. Rev. Lett. **71**, 1994 (1993).
[4] K. J. Schafer, Phys. Rev. Lett. **71**, 1599 (1993).
[5] N. B. Delone and V. P. Krainov, J. Opt. Soc. Am. B **8**, 1207 (1991).
[6] L. Arissian, C. Smeenk, F. Turner, C. Trallero, A. V. Sokolov, D. M. Villeneuve, A. Staudte, and P. B. Corkum, Phys. Rev. Lett. **105**, 133002 (2010).
[7] G. L. Yudin and M. Y. Ivanov, Phys. Rev. A **64**, 013409 (2001).
[8] M. Y. Ivanov, M. Spanner, and O. Smirnova, J. Mod. Opt. **52**, 165 (2005).
[9] N. Dudovich, J. Levesque, O. Smirnova, D. Zeidler, D. Comtois, M. Y. Ivanov, D. M. Villeneuve, and P. B. Corkum, Phys. Rev. Lett. **97**, 253903 (2006).
[10] E. Goulielmakis, V. S. Yakovlev, A. L. Cavalieri, V. Pervak, A. Apolonski, R. Kienberger, U. Kleineberg, and F. Krausz, Science **317**, 769 (2007).
[11] D. Herrmann, L. Veisz, R. Tautz, F. Tavella, K. Schmid, V. Pervak, and F. Krausz, Opt. Lett. **34**, 16 (2009).
[12] Z. Chang, Phys. Rev. A **70**, 043802 (2004).
[13] G. Sansone, E. Benedetti, F. Calegari, C. Vozzi, L. Avaldi, R. Flammini, L. Poletto, P. Villoresi, C. Altucci, R. Velotta, S. Stagira, S. De Silvestri, and M. Nisoli, Science **314**, 443 (2006).
[14] P. B. Corkum, N. H. Burnett, and M. Y. Ivanov, Opt. Lett. **19**, 1870 (1994).
[15] P. Tzallas, E. Skantzakis, C. Kalpouzos, E. P. Benis, G. D. Tsakiris, and D. Charalambridis, Nat. Phys. **3**, 846 (2007).
[16] Z. Chang, Phys. Rev. A **76**, 051403(R) (2007).
[17] H. Mashiko, S. Gilbertson, C. Li, S. D. Khan, M. M. Shakya, E. Moon, and Z. Chang, Phys. Rev. Lett. **100**, 103906 (2008).
[18] X. Feng, S. Gilbertson, H. Mashiko, H. Wang, S. D. Khan, M. Chini, Y. Wu, K. Zhao, and Z. Chang, Phys. Rev. Lett. **103**, 183901 (2009).
[19] G. Sansone, L. Poletto, and M. Nisoli, Nat. Photonics **5**, 655 (2011); C. Altucci, J. W. G. Tisch, and R. Velotta, J. Mod. Opt. **58**, 1585 (2011).
[20] K. S. Budil, P. Salieres, A. L'Huillier, T. Ditmire, and M. D. Perry, Phys. Rev. A **48**, R3437 (1993).
[21] P. Antoine, A. L'Huillier, M. Lewenstein, P. Salieres, and B. Carre, Phys. Rev. A **53**, 1725 (1996).
[22] C. Altucci, V. Tosa, and R. Velotta, Phys. Rev. A **75**, 061401(R) (2007).
[23] G. Sansone, Phys. Rev. A **79**, 053410 (2009).
[24] N. I. Shvetsov-Shilovski, S. P. Goreslavski, S. V. Popruzhenko, and W. Becker, Phys. Rev. A **77**, 063405 (2008).
[25] P. Salieres, B. Carre, L. Le Deroff, F. Grasbon, G. G. Paulus, H. Walther, R. Kopold, W. Becker, D. B. Milosevic, A. Sapera, and M. Lewenstein, Science **292**, 902 (2001).
[26] Z. Chang, in *Fundamentals of Attosecond Optics*, 1st ed. (CRC, Boca Raton, FL, 2011), p. 251.
[27] H. Xu, H. Xiong, B. Zeng, W. Chu, Y. Fu, J. Yao, J. Chen, X. Liu, Y. Cheng, and Z. Xu, Opt. Lett. **35**, 4 (2010).
[28] F. He, C. Ruiz, and A. Becker, Opt. Lett. **32**, 21 (2007).
[29] S. D. Khan, Y. Cheng, M. Möller, K. Zhao, B. Zhao, M. Chini, G. G. Paulus, and Z. Chang, Appl. Phys. Lett. **99**, 161106 (2011).